Journal of Power Sources 208 (2012) 322–327

Contents lists available at SciVerse ScienceDirect

Journal of Power Sources

journal homepage: www.elsevier.com/locate/jpowsour

High efficiency energy harvesting from microbial fuel cells using a synchronous boost converter

Jae-Do Park[a,*], Zhiyong Ren[b]

[a] Department of Electrical Engineering, University of Colorado Denver, Denver, CO 80217, United States
[b] Department of Civil Engineering, University of Colorado Denver, Denver, CO 80217, United States

ARTICLE INFO

Article history:
Received 20 January 2012
Received in revised form 8 February 2012
Accepted 11 February 2012
Available online 20 February 2012

Keywords:
Microbial fuel cell (MFC)
Energy harvesting
DC/DC converter
Synchronous boost converter

ABSTRACT

Microbial fuel cells (MFCs) convert chemical energy stored in biodegradable substrates into direct electricity, which can be used to power remote sensors or offset the energy used during wastewater treatment. Power electronic converters have been developed to replace external resistors and harvest and store energy from MFCs, which is a significant improvement in MFC studies because external resistors only demonstrate power generation potential without actually capturing usable energy. However, the efficiency of conventional diode based energy harvester is low due to the high power loss of the diode. This study presents a synchronous boost converter based MFC energy harvester using a P-channel MOSFET, which improved the converter efficiency by 73%, from 43.8% to 75.9%. A modified hysteresis controller was developed to provide precise control during energy harvesting and operating and also prevented reverse current flows.

1. Introduction

Worldwide concerns on environmental pollution, energy depletion, and climate change are driving the development of sustainable energy alternatives. The direct electricity production from organic materials via microbial fuel cells (MFCs) offers great economic and environmental benefits because the energy produced offsets the energy consumption associated with wastewater treatment and reduces maintenance cost for remote sensing networks [1–3]. MFCs use electrochemically active bacteria to extract the electrons from biodegradable substrates and produce direct electric current. Static external resistors have been generally used in MFC studies to measure the output power, and polarization data can be obtained by applying a series of different resistors to the output or by an electrochemical scan using a potentiostat [4–7].

Although resistors can characterize the MFC power generation potential, they cannot be harvesting devices because the generated electricity is dissipated into heat instead of being utilized or stored. The open circuit voltage (OCV) of an air-cathode MFC is around 0.8 V due to thermodynamic limitations [4,8], and it is difficult for an MFC to directly support a practical load even at the maximum power generating point due to the low voltage and current level. The maximum output power can be generated when the applied external resistance is equal to the system internal resistance, or when the output voltage is identical with the internal voltage drop [3,6]. It is also difficult to develop very large-sized reactors for higher power because the generation power density is not a linear function of the reactor size, and stacks of MFCs may have voltage reversal problems due to the unequal performance of different units. A recent study showed that parallel charging of multiple capacitors can avoid potential voltage reversal while series discharging could increase MFC output voltage [8,9]. Charge pumps have also been used to harvest MFC energy [7,10,11], but they can only capture the energy passively without enough controllability on operating conditions [12,13].

Compared to the current harvesting approaches that passively rely on the MFC to provide energy, DC/DC switching converters can actively extract energy from MFCs by high frequency switching action and therefore have advantages in capturing practically usable energy and shaping it to a practical form [12]. We have demonstrated that the operating voltage can be easily maintained at the maximum power point and the output voltage can be boosted to standard level of 1.5 V or 3.3 V using a separate boost converter to support electronic loads. However, we also found that the efficiency is low because of the significant energy loss due to diode forward voltage drop. Unlike the resistive voltage drop, the diode forward voltage drop, which is the potential difference between anode and cathode of diode when it is conducting, varies only a little with the current. Hence, although a diode is simple and requires no control circuitry, its 0.4 V forward voltage drop is significant considering the MFC operating voltage around 0.3 V.

* Corresponding author. Tel.: +1 303 352 3743; fax: +1 303 556 2383.
E-mail address: jaedo.park@ucdenver.edu (J.-D. Park).

0378-7753/$ – see front matter © 2012 Elsevier B.V. All rights reserved.
doi:10.1016/j.jpowsour.2012.02.035

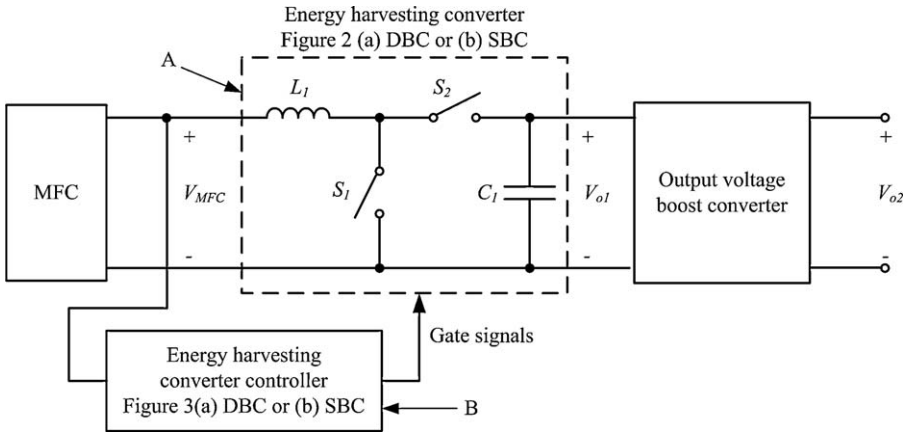

Fig. 1. Block diagram of boost converter based MFC energy harvesting system. L_1: energy storing inductor; S_1: harvesting converter main switch; S_2: harvesting converter output switch; C_1: energy storage capacitor.

In this study, we developed a synchronous boost converter (SBC) based energy harvesting system that can remarkably increase energy conversion efficiency. The proposed converter utilizes a P-channel MOSFET to replace the diode in the traditional diode based boost converter (DBC). A modified hysteresis controller was also integrated into the system to gain better control of the operating voltage and MOSFET switches.

2. Materials and methods

2.1. Boost converter based MFC energy harvesting system

A harvesting system for multiple MFCs using DC/DC converters and hysteresis circuit was presented in our previous work [12]. The system consists of two layers of DC/DC converters. The first converter extracts energy from the MFC, and the second layer converter boosts the voltage to a suitable level for the load. Fig. 1 shows the block diagram of the boost converter based energy harvesting system. Although this harvesting scheme can control the operating point at the maximum power point, it suffers from the high conduction loss if a diode is used as S_2, as shown in Fig. 2(a). In this paper, we focus on developing a new harvesting converter to significantly improve system energy conversion efficiency (Fig. 1 box A).

Implementation of a diode based boost converter is straightforward because the diode automatically opens when it is reverse biased and does not allow a reverse flow except a small reverse recovery current. The effect of reverse recovery can be negligible if a fast recovery Schottky diode is used. However, due to high power loss, the diode was replaced with a metal oxide semiconductor field effect transistor (MOSFET) Q_2, which can be seen in Fig. 2(b), and it is called synchronous boost converter because the MOSFET Q_2 is controlled synchronously with Q_1. Compared to diodes, the MOSFET has significantly low conduction loss due to its low on-state resistance. They are toggled complimentarily, i.e., Q_1 ON/Q_2 OFF and Q_1 OFF/Q_2 ON. It should be noted that the MOSFET has an intrinsic body diode built in as well. Although the SBC can achieve higher efficiency due to its low conduction loss, it requires complex control circuitry because the secondary switch Q_2 is a "floating" or "high-side" switch that has its source terminal connected to the output capacitor C_1. P-channel MOSFET has advantage over N-channel MOSFET, because the gate voltage can be referenced on capacitor voltage which is slowly changing. When a P-channel MOSFET is used for Q_2, the controller needs to apply $V_{C1} - V_{GSth}$ to gate terminal to turn it on. V_{GSth} is the MOSFET turn-on threshold voltage. Another difficulty for the SBC control is the timing of Q_2 turn-off. Unlike the diode, the MOSFET conducts bidirectional currents. Hence, a negative inductor current will flow if the switch Q_2 is not turned off when the current reduces to zero, which means the energy in the capacitor will be discharged through Q_2 and L_1 to MFC side. This reverse power flow drastically reduces the harvesting efficiency.

In this paper, a synchronous boost converter integrated with a modified hysteresis controller is developed to improve the harvesting efficiency. A floating gate signal generator for Q_2 is developed and the timing control circuitry to ensure Q_2 turn-off at a right timing to avoid reverse power flow is integrated in the hysteresis controller.

2.2. Hysteresis controller for operating voltage and switch control

The hysteresis controller in [12] generates gating signal for Q_1 in Fig. 2(a) to control the operating voltage at the maximum

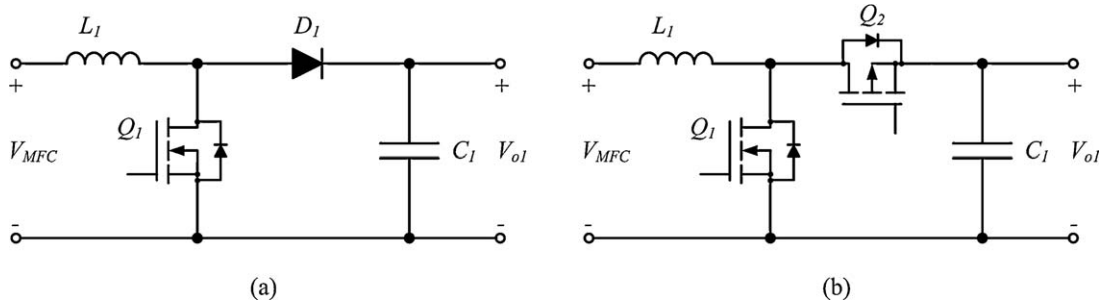

Fig. 2. Schematics of energy harvesting converters for Fig. 1 box A. (a) Diode based boost converter (DBC). (b) P-ch MOSFET based synchronous boost converter (SBC). L_1: energy storing inductor; Q_1: harvesting converter main MOSFET switch; D_1: harvesting converter output diode; Q_2: harvesting converter output MOSFET; C_1: energy storage capacitor.

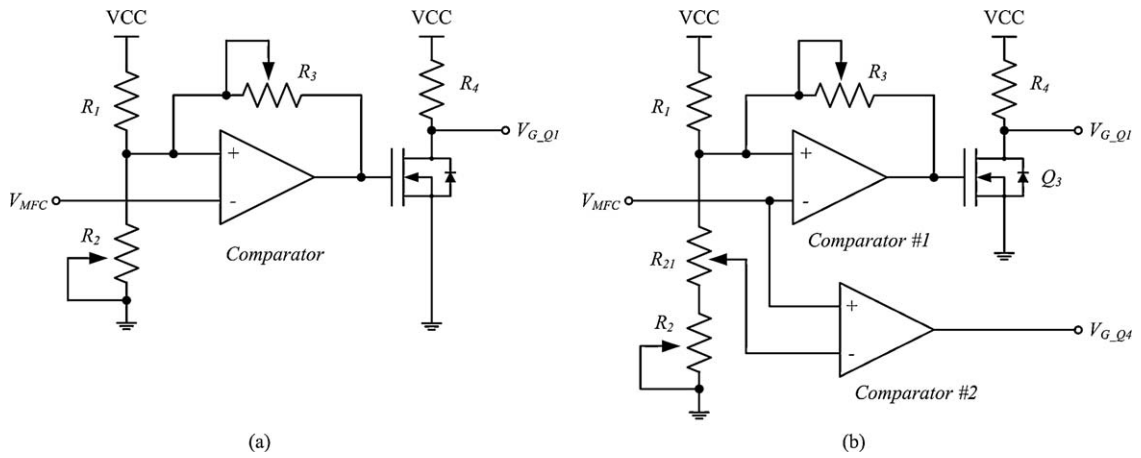

Fig. 3. Schematic of harvesting converter controller in Fig. 1 box B. (a) For DBC. (b) For SBC. VCC: voltage reference; V_{MFC}: MFC output voltage; $V_{G.Q1}$: harvesting converter main MOSFET gate signal; $V_{G.Q4}$: harvesting converter output MOSFET gate signal.

power point of the MFC and ensure enough recovery time for MFC. The energy harvester has two operation modes: CHARGE and DISCHARGE mode. The energy is extracted from the MFC during the CHARGE mode and stored in the inductor L_1. The MFC voltage V_{MFC} decreases in this mode. In DISCHARGE mode, the switch Q_1 is off to get the energy stored in inductor L_1 discharged to the storage capacitor C_1 through D_1. The MFC voltage increases and the MFC output current decreases.

The switch Q_1 is toggled when the MFC voltage reaches lower threshold and upper threshold in the CHARGE mode and DISCHARGE mode, respectively. The frequency of power extraction or the mode change between CHARGE and DISCHARGE depends on the MFC's condition so that the MFC voltage can be maintained in the hysteresis voltage band, $V_{thH} - V_{thL}$. As well as capturing right amount of energy to maintain the voltage at the appropriate level, the hysteresis controller provides enough recovery time for the MFC reactor. If the harvester extracts energy without proper recovery time, the MFC voltage could collapse. The schematic of DBC harvester controller is shown in Fig. 3(a).

For SBC, the hysteresis controller should generate a gating signal for Q_2 as well. It needs to be toggled synchronously with Q_1, but it should be turned off properly to avoid negative current. For the Q_2 gate signal, additional comparator has been added in the hysteresis circuit. To ensure that Q_2 turns off slightly earlier than Q_1 turn-on, an additional potentiometer is added in the circuit to provide an additional voltage threshold. The modified hysteresis controller is shown in Fig. 3(b) and it can be seen that the negative terminal of *comparator #2* is connected to the slider terminal of potentiometer R_{21}, so that the *comparator #2* operates with a slightly lower threshold voltage than *comparator #1* because $R_{21\text{-slider}}$ is smaller than R_{21}. The threshold voltages are given as follows:

$$V_{thH} = V_{CC} \cdot \frac{R_2 + R_{21}}{(R_2 + R_{21}) + (R_1 // R_3)} \quad (1)$$

$$V_{thL} = V_{CC} \cdot \frac{R_2 + R_{21} // R_3}{R_1 + ((R_2 + R_{21}) + R_3)} \quad (2)$$

$$V'_{thH} = V_{CC} \cdot \frac{R_2 + R_{21\text{-slider}}}{((R_2 + R_{21}) + (R_1 // R_3)} \quad (3)$$

$$V'_{thL} = V_{CC} \cdot \frac{(R_2 + R_{21\text{-slider}}) // R_3}{R_1 + ((R_2 // R_{21}) // R_3)} \quad (4)$$

where V_{thH} and V_{thL} are thresholds for Q_1 and V'_{thH} and V'_{thL} are additional thresholds that are slightly lower.

3. Experimental

3.1. Synchronous boost converter

A prototype synchronous boost controller has been implemented. The N-channel MOSFET Q_1 uses Vishay SI3460 and P-channel MOSFET Q_2 uses Vishay SI4483. The on-resistance of these MOSFETs is 27 mΩ and 15.3 mΩ at 4.5 V V_{GS}, respectively. National Semiconductor's comparator LMC7215 is chosen for low power consumption. The LMC7215 consumes only 1 μA of power supply current. An off-the-shelf pulse transformer IT246 (Schaffner EMC) is used for floating switch gate driver. The turn-ratio of the transformer is 1:2. Also a Schottky diode 1N5711 has been used for DBC for comparison. The forward voltage V_F is 0.41 V with 1 mA I_F. A 110 mH inductor CST206-3A has been used for the experiments in this paper. Single 2.5 V, 1 F super capacitor has been used for energy storage. The developed energy harvester and the MFC reactor are shown in Fig. 4.

3.2. MFC reactor

A two-chamber cubic-shaped MFC reactor with 7 cm chamber diameter (Fig. 4) was used for the experiments in this paper. The reactor used a cation exchange membrane (CEM, CMI 7000, Membranes International, NJ) to separate the anode and cathode chambers that had 140 mL of chamber volume. Heat treated

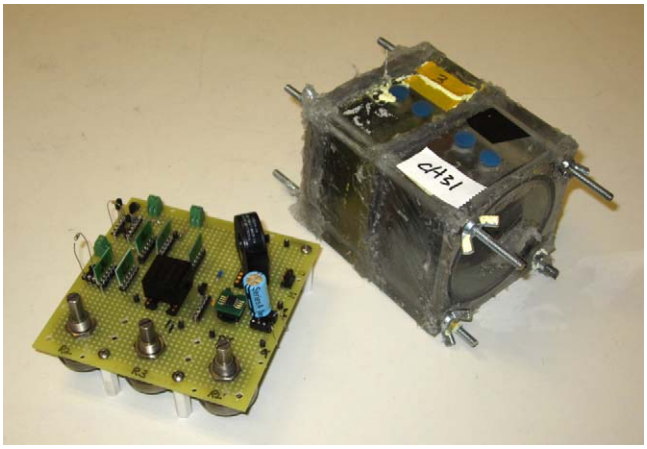

Fig. 4. Experiment setup. The energy harvester and two-chamber MFC reactor. The harverter contains DBC and SBC.

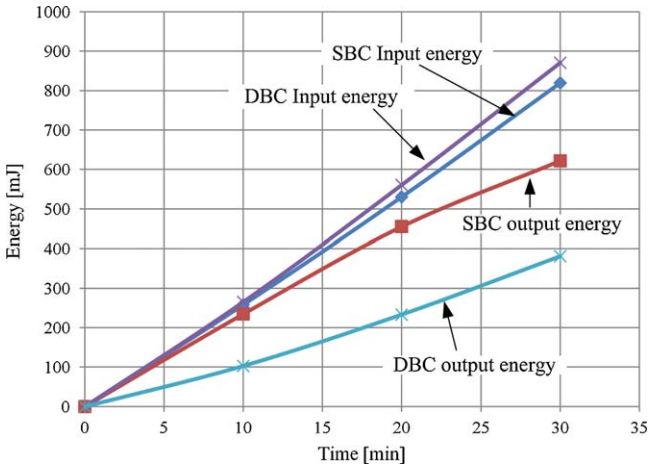

Fig. 5. Experimental result: input/output energy of DBC and SBC based energy harvester.

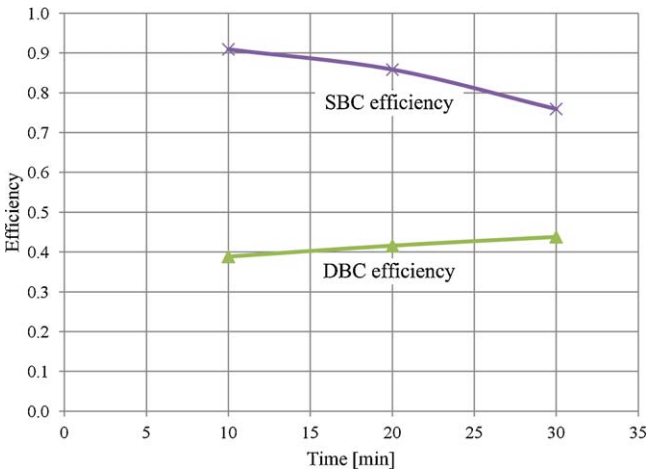

Fig. 6. Experimental result: efficiency of DBC and SBC based energy harvester.

graphite brushes and plain carbon paper was selected for the anode and cathode material, respectively [14]. The cathode effects on system performance were minimized by using the phosphate (50 mM) buffered ferricyanide (50 mM) as the catholyte. Reactors were inoculated using effluent from another MFC operated for more than 1 year in the same lab. Anolyte medium solution contained 1.25 g L^{-1} CH_3COONa, 0.31 g L^{-1} NH_4Cl, 0.13 g L^{-1} KCl, 3.321 g L^{-1} $NaH_2PO_4{\cdot}2H_2O$, 10.317 g L^{-1} $Na_2HPO_4{\cdot}12H_2O$, 12.5 mL L^{-1} mineral solution, and 5 mL L^{-1} vitamin [15]. The reactor was operated in fed-batch mode at room temperature and refilled with new medium solution as required to maintain the electrical characteristics.

4. Results and discussion

4.1. Efficiency improvement by SBC

Energy harvesting from the lab-scale two-chamber MFC reactor for 30 min was performed using a DBC and the proposed SBC for comparison. The MFC voltage V_{MFC}, MFC current I_{MFC} and output capacitor voltage V_{C1} of 2.5 V 1 F supercapacitor were measured and used for calculation of input energy E_{in} generated by MFC for time duration T, which is 30 min, output energy E_{out} and efficiency η, which can be given as follows:

$$E_{in} = \hat{V}_{MFC} \times \hat{I}_{MFC} \times T \tag{5}$$

$$E_{out} = \frac{1}{2} C_1 V_{C1}^2 \tag{6}$$

$$\eta = \frac{E_{out}}{E_{in}} \tag{7}$$

where $\hat{X}$ denotes average value. After each 30-min harvesting operation, the SBC stored 621 mJ in capacitors out of the 820 mJ harvested from the MFC, while the DBC stored 381 mJ out of 870 mJ (Fig. 5). Compared with the DBC, the SBC harvesting controller improved the overall efficiency from 43.8% to 75.9% (Fig. 6).

The overall efficiency is given as

$$\eta = \frac{E_{out}}{E_{in}} = \frac{E_{out}}{E_{out} + E_{loss}} \tag{8}$$

where E_{loss} is the total loss including the rectifier loss. The diode loss is dominant in the DBC harvester, which can be calculated as follows:

$$E_{loss\_diode} \approx V_F \times \hat{I}_{MFC} \times T_{diode} = 332.8\,\text{mJ} \tag{9}$$

The MOSFET loss can be given as

$$E_{loss\_MOSFET} \approx R_{DS\_ON} \times \hat{I}_{MFC} \times T_{MOSFET} = 0.018\,\text{mJ} \tag{10}$$

which shows that the SBC based harvester eliminated the diode loss and increased the harvested energy. It should be noted that the reactor generated slightly different energy in each experiment and the SBC harvested more energy even from a smaller input energy. In Fig. 7, the MFC voltage/current and output capacitor voltage of DBC and SBC based harvester is shown. The MFC voltage was maintained at 315 mV and the reactor generates slightly higher current for DBC experiment. It can be clearly seen that the SBC output voltage is higher than DBC output due to the higher harvested energy.

The efficiency of the SBC was quite high at the beginning when the capacitor voltage is low and it decreased as the capacitor voltage increases. The energy harvesting converter works as a current source with a large output capacitance, unlike conventional DC/DC converters which controls the output voltage [17]. The efficiency drop with output voltage increase is inevitable because the power injected into the capacitor decreases as capacitor voltage increases. The average capacitor charging current I_{Q2} is given as follows because it charges the capacitor only in DISCHARGE mode.

$$\hat{I}_{Q2} = (1 - D)\hat{I}_{MFC} \tag{11}$$

where D is the duty ratio for Q_1, which is the ratio of turn-on time to the total switching period. The power injection experiences more resistance because of the increasing capacitor voltage and

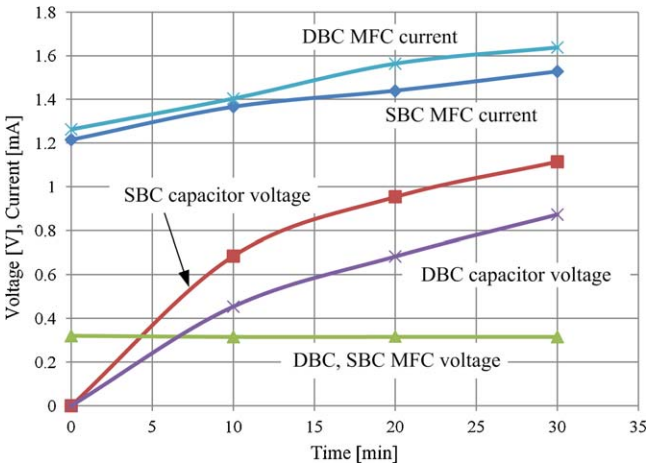

Fig. 7. Experimental result: MFC voltage, MFC current, and capacitor voltage of DBC and SBC based energy harvester.

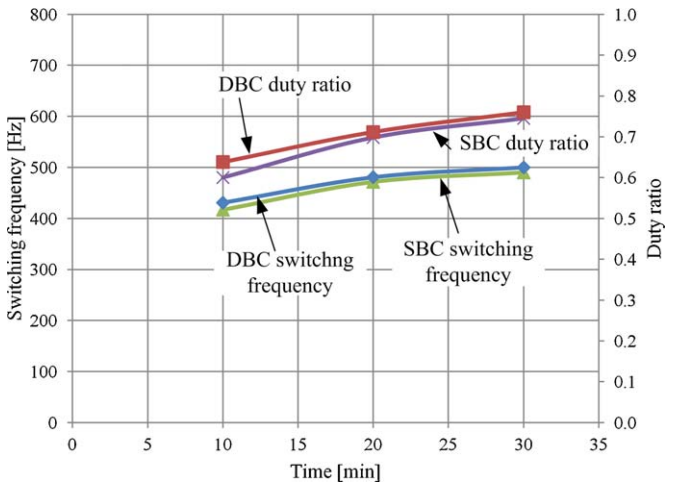

Fig. 8. Experimental result: main switch Q_1 duty ratio and switching frequency of DBC and SBC based energy harvester.

this makes the switching frequency and Q_1 duty ratio increase as can be seen in Fig. 8, which reduces discharging period $(1-D)/F_{sw}$. Consequently the average capacitor charging current and harvested energy decreases. Therefore, the system should be carefully designed not to have too high output voltage, taking the load current into consideration. The experiments in this paper have been performed in no load condition. The output voltage of harvester does not need to be high because final output voltage to the actual load is boosted by the converter in the second layer in Fig. 1. On the other hand, the diode-based harvester's efficiency increased with the output voltage. This is because the initial efficiency is too low due to the constant diode forward voltage, compared to the constant resistance of MOSFET.

4.2. Harvester operation

The voltage difference between V_{thH} for Q_1 and V'_{thH} for Q_2, that determines the time advance for Q_2 turn-off, can be adjusted by potentiometer R_{21}, but changing slider position of R_{21} does not affect V_{thH} and V_{thL} because the resistance between R_2 and R_1 is not changed. Hence, the time for advanced Q_2 turn-off can be adjusted independently to Q_1 thresholds. It should be noted that the MFC voltage cannot reach the lower threshold V'_{thL} because the operating mode changes at V_{thL} and V_{MFC} changes its direction. For the Q_2 gate driver, a transformer and an N-channel MOSFET is used to generate a floating voltage with the capacitor voltage [16].

Typical waveforms of DBC and SBC based harvester operation are shown in Fig. 9(a) and (b), respectively. The operation mode, MFC voltage, voltage across Q_2, and currents in the continuous conduction mode (CCM) and discontinuous conduction mode (DCM) are shown. In the SBC harvester, the voltage drop across Q_2, V_{DS_Q2}, is considerably smaller due to the low on-resistance compared to the constant diode forward voltage drop V_F. However, if a reverse discharge from C_1 in DCM is not prevented, the energy loss is incomparably higher than energy gain by efficiency improvement due to low on-state voltage V_{DS_Q2}. The prevention of reverse current flow is shown in the circle. A DBC can inherently avoid reverse current flow in both CCM and DCM because the bias is automatically reversed as converter's operating mode changes, but diode forward voltage V_F makes the conduction loss significantly high.

The detailed experimental waveforms of a DBC and the proposed SBC are shown in Fig. 10(a) and (b), respectively. For both harvesting controllers, the MFC voltage is maintained at 315 mV average and the hysteresis band is set for the reactor to operate in marginal DCM. For diode-based boost converter experiment, it can be seen that there is no reverse current flow but the diode forward voltage V_F is 0.4 V. On the contrary, the SBC has a very low on-state voltage, but the output P-channel MOSFET needs to be carefully controlled to avoid negative current flow. The proposed reverse power flow prevention scheme turns Q_2 off in advance and makes the current flow through the body diode of Q_2 at the end of the DISCHARGE mode, where the increased voltage can be seen. This could slightly decrease the efficiency gain, but the increased voltage at the end of the on-state of Q_2 assures that the reverse power flow is prevented.

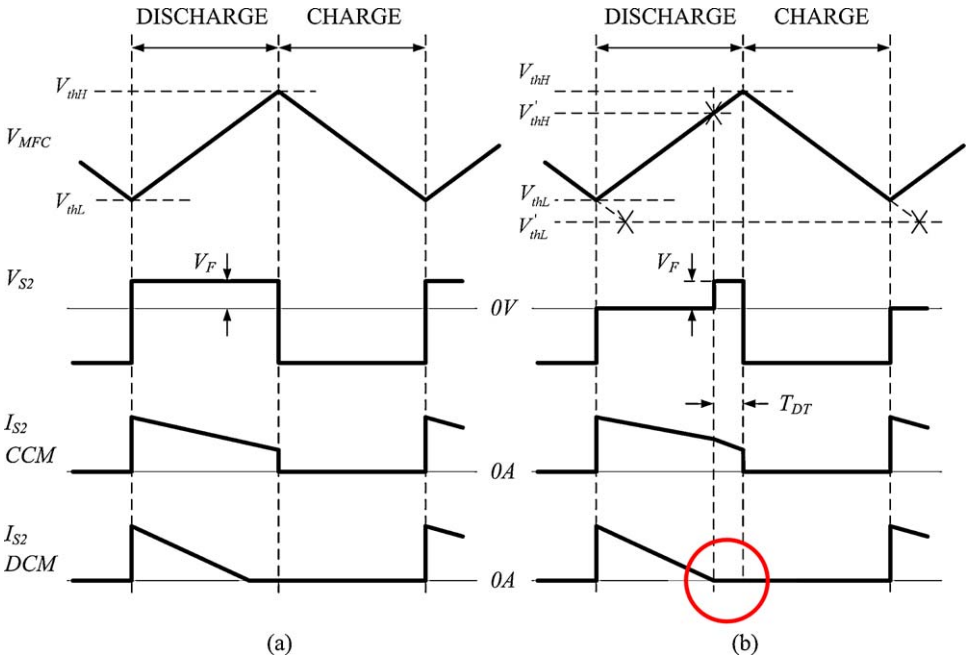

Fig. 9. Waveforms of energy harvesting converter. (a) DBC. (b) SBC. From top, MFC voltage, voltage across S_2 (D_1 for DBC, Q_2 for SBC), S_2 current in continous conduction mode, S_2 current in discontinous conduction mode.

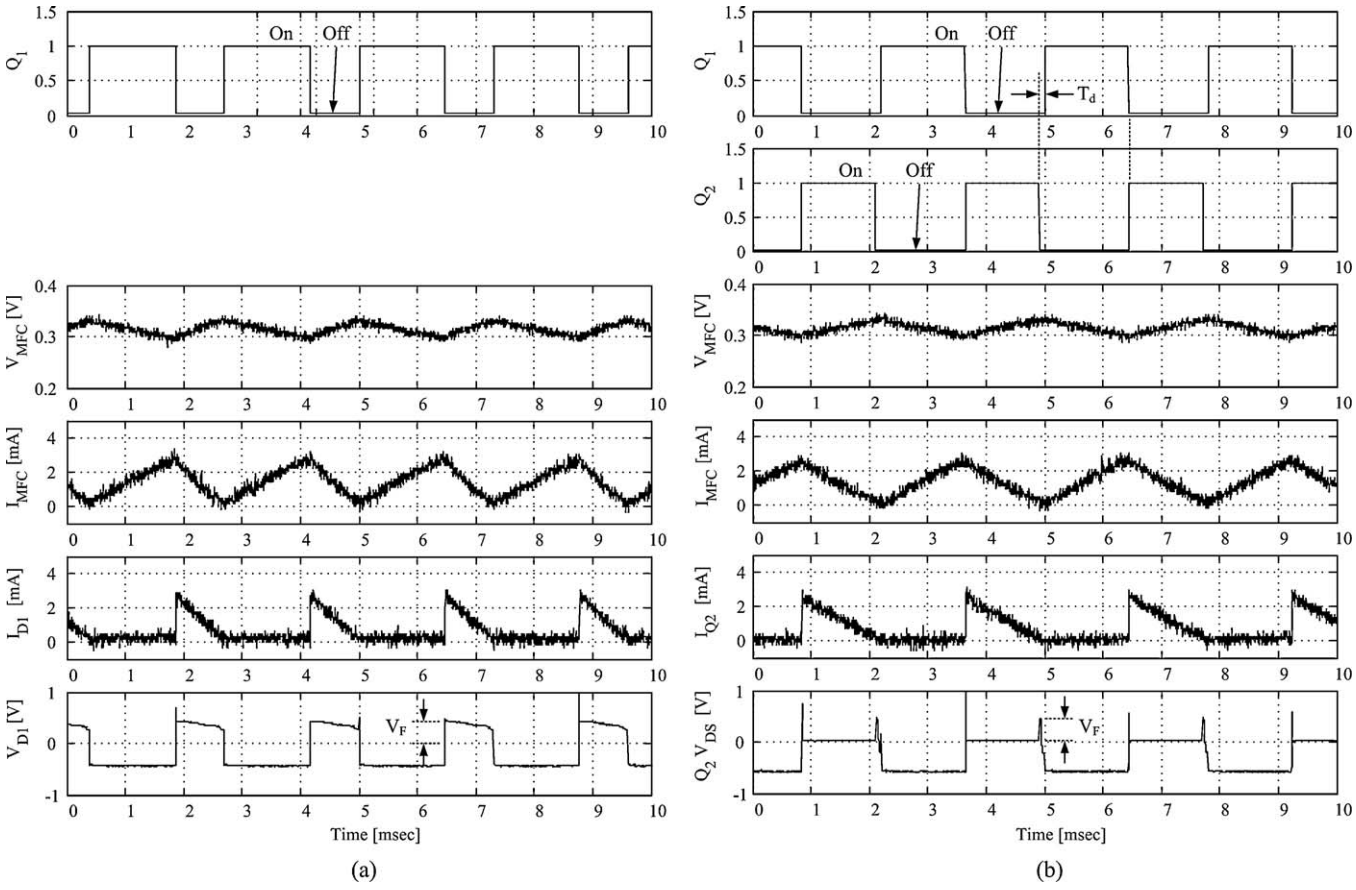

Fig. 10. Experimental result: detailed operation of (a) DBC and (b) SBC based energy harvester. From top, Q_1 status, Q_2 status (SBC only), MFC voltage, MFC current, S_2 current, and voltage across S_2.

Due to the low energy capacity of the MFC reactor under test, the control circuitry was powered by an external power supply for continuous monitoring. Also, the circuitry has not been optimized for minimal power consumption in this proof-of-concept study. However, low-power parts and a CMOS ASIC would readily accommodate the proposed method for minimal power consuming and self-sustainable implementation, and self-sustained circuitry is currently under development.

5. Conclusions

In this paper, a synchronous boost converter was developed for more efficient energy harvesting from MFCs. Compared to the conventional diode based boost converter, the synchronous boost converter based harvester increased harvesting efficiency by 73%. A modified hysteresis controller was utilized for the operating point and output switch control, and a simple but effective reverse power flow prevention scheme using additional potentiometer and comparator was integrated with the harvesting controller, all of which significantly improved harvesting effectiveness.

Acknowledgements

This work was supported by University of Colorado Denver College of Engineering and Applied Science (Park) and the Office of Naval Research (ONR) under Award N000140910944 (Ren). Authors thank Heming Wang for providing the MFC reactors.

References

[1] F. Zhang, L. Tian, Z. He, J. Power Sources 196 (2011) 9568–9573.
[2] B.E. Logan, Appl. Microbiol. Biotechnol. 85 (2010) 1665–1671.
[3] Z. Ren, H. Yan, W. Wang, M. Mench, J. Regan, Environ. Sci. Technol. 45 (2011) 2435–2441.
[4] L. Woodward, M. Perrier, B. Srinivasan, R.P. Pinto, B. Tartakovsky, AIChE J. 56 (2010) 2742–2750.
[5] K. Jacobson, D. Drew, Z. He, Bioresour. Technol. 102 (2010) 376–380.
[6] R.P. Pinto, B. Srinivasan, S.R. Guiot, B. Tartakovsky, Water Res. 45 (2011) 1571–1578.
[7] A. Dewan, C. Conovan, H. Deukhyoun, H. Beyenal, J. Power Sources 195 (2010) 90–96.
[8] Y. Kim, M.C. Hatzell, A.J. Hutchinson, B.E. Logan, Energy Environ. Sci. 4 (2011) 4662–4667.
[9] S. Oh, B. Logan, J. Power Sources 167 (2007) 11–17.
[10] C. Donovan, A. Dewan, H. Peng, D. Heo, H. Beyenal, J. Power Sources 196 (2011) 1171–1177.
[11] A. Meehan, G. Hongwei, Z. Lewandowski, IEEE Trans. Power Electronics (2011) 176–181.
[12] J. Park, Z. Ren, Proceedings of IEEE Energy Conversion Congress and Exposition, 2011, pp. 3852–3858.
[13] J. Park, Z. Ren, J. Power Sources (2012), doi:10.1016/j.jpowersour.2012.01.053.
[14] H. Wang, Z. Wu, A. Plaseied, P. Jenkins, L. Simpson, C. Engtrakul, Z. Ren, J. Power Sources 196 (2011) 7465–7469.
[15] H. Luo, P. Jenkins, Z. Ren, Environ. Sci. Technol. 45 (2011) 340–344.
[16] International Rectifier, Application Note AN-950, 2000.
[17] R. Erickson, D. Maksimovic, Fundamentals of Power Electronics, 2nd ed., 2001.